NEW APPROACH TO MEASURING QUARK–GLUON JETS AT THE LHC*

Petr Baroň

Institute of Nuclear Physics Polish Academy of Sciences
Radzikowskiego 152, 31-342 Kraków, Poland
Petr.Baron@ifj.edu.pl

Michael H. Seymour

Lancaster-Manchester-Sheffield Consortium for Fundamental Physics
Department of Physics and Astronomy
University of Manchester, M13 9PL, U.K.
Michael.Seymour@manchester.ac.uk

Andrzej Siódmok

Jagiellonian University, Łojasiewicza 11, 30-348 Kraków, Poland
Andrzej.Siodmok@uj.edu.pl

Received 15 January 2024, accepted 20 January 2024, published online 11 March 2024

This paper describes a novel method for measuring quark/gluon jet properties at the Large Hadron Collider (LHC) at CERN. The advantage of this method is the use of data collected at different energies during LHC operation, allowing these data sets to be combined to obtain distributions of jet properties categorized into quark- and gluon-jet samples on a statistical basis. The method is presented with various angularity observables, and the search for the most useful observables is performed.

DOI:10.5506/APhysPolBSupp.17.2-A9

1. Introduction

When high-energy quarks or gluons are produced in a particle collision, they cannot exist as isolated particles due to the nature of the strong force. Instead, they quickly undergo a process called parton showering and hadronization, resulting in a stream of particles moving in roughly the same direction. This collimated spray of particles is called a jet and is tightly connected to the jet reconstruction algorithm. Having a method to distinguish jets initiated by quarks or gluons is crucial for improving the separation of

* Presented by P. Baroň at the XLV International Conference of Theoretical Physics "Matter to the Deepest", Warsaw, Poland, 17–22 September, 2023.

signal from background in various processes in high-energy physics experiments. Detailed aspects and additional studies of the presented method are shown in [1].

This study focuses on five generalised angularities λ_β^κ of jets named depending on the choice of exponents κ and β [2]:

— multiplicity — λ_0^0,
— p_{T}^D — λ_0^2,
— LHA — $\lambda_{0.5}^1$,
— width — λ_1^1, and
— mass — λ_2^1.

The exponents κ and β of each angularity λ_β^κ enter the calculation

$$\lambda_\beta^\kappa = \sum_{i \in \mathrm{jet}} z_i^\kappa \theta_i^\beta \,, \tag{1}$$

where the sum loops over the jet constituents i, z_i stands for transverse momentum fraction of the jet constituent $z_i \equiv \frac{p_{\mathrm{T}i}}{\sum_{j \in \mathrm{jet}} p_{\mathrm{T}j}} \in [0,1]$, and $\theta_i \equiv \frac{R_{i\hat{n}}}{R} \in [0,1]$ is calculated using $R_{i\hat{n}}$ — the rapidity-azimuth distance to the jet axis, and R is the jet-radius parameter.

2. Sets of jets

The sets of jets from dijet events $pp \to jj$ were produced using two event generators Herwig 7.2.2 [3, 4] (MMHT2014lo68cl PDF set [5]) and Pythia 8.240 [6, 7] (NNPDF2.3 QCD+QED LO PDF set [8]) at four different centre-of-mass energies $\sqrt{s} = 900$ GeV, 2.36 TeV, 7 TeV, 13 TeV as they would be collected at the Large Hadron Collider (LHC) at CERN. For the reconstruction, the Anti-k_{T} algorithm [9] implemented in the FastJet package [10, 11] with radii $R = 0.2$, 0.4, 0.6, 0.8, and 1.0 was used. Two transverse momentum p_{T} criteria of the jets were applied

$$p_{\mathrm{T\,sublead}} / p_{\mathrm{T\,lead}} > 0.8 \tag{2}$$

and

$$(p_{\mathrm{T\,lead}} + p_{\mathrm{T\,sublead}})/2 > p_{\mathrm{T}}^{\mathrm{cut}} \,, \tag{3}$$

where $p_{\mathrm{T\,lead}}$ is the transverse momentum of the leading jet and $p_{\mathrm{T\,sublead}}$ is the transverse momentum of the subleading jet. Four different transverse momentum cuts $p_{\mathrm{T}}^{\mathrm{cut}} = 50$, 100, 200, and 400 GeV were studied. In addition to directly measuring the angularities, the impact of jet grooming (see *e.g.* [12–15]) was tested using a modified mass drop tagger (MMDT) with $\mu = 1$ [12, 16] (equivalently, soft drop declustering with $\beta = 0$ [17]) and $z_{\mathrm{cut}} = 0.1$.

3. Quark and gluon angularities

Once having a collection of jets at four different energies 900 GeV, 2.36 TeV, 7 TeV, and 13 TeV, the five types of jet angularities λ were calculated as a function of jet $p_{\mathrm{T}}^{\mathrm{cut}}$ and radius R according to equation (1). The example of jet angularities λ_0^0 (multiplicities, $R = 0.4$, $p_{\mathrm{T}}^{\mathrm{cut}} = 100$ GeV) is shown in figure 1 by the green dashed line for the energy of 900 GeV and by the black line for the energy of 13 TeV. Each distribution λ_0^0 at the energies of 900 GeV and 13 TeV is composed of a different abundance of quark and gluon jets, which can be generally written for one of five jet angularities λ as

$$\lambda = f\lambda_g + (1-f)\lambda_q\,, \tag{4}$$

where f is the fraction of gluon jets, $(1-f)$ fraction of quark jets, λ_g gluon angularity, and λ_q quark angularity. The study aims to extract quark λ_q and gluon λ_g angularities and the key idea is to use jet angularities derived (or ideally measured) at two distinct energies coming back to the example in figure 1, we could write

$$\lambda^{900} = f^{900}\lambda_g + \left(1-f^{900}\right)\lambda_q\,, \tag{5}$$

$$\lambda^{13000} = f^{13000}\lambda_g + \left(1-f^{13000}\right)\lambda_q\,, \tag{6}$$

where the upper script refers to the two distinct energies of 900 GeV and 13 TeV. Assuming quark λ_q and gluon λ_q angularities are independent of the energy, one can extract quark angularity λ_q,

$$\lambda_q = \frac{f^{13000}\lambda^{900} - f^{900}\lambda^{13000}}{f^{13000} - f^{900}}\,, \tag{7}$$

and gluon angularity λ_g,

$$\lambda_g = \frac{\left(1-f^{900}\right)\lambda^{13000} - \left(1-f^{13000}\right)\lambda^{900}}{f^{13000} - f^{900}}\,. \tag{8}$$

The fractions f^{900} and f^{13000} are taken from the simulation and will be discussed in the following Section 4. Examples of quark λ_q and gluon λ_g angularities (multiplicities) are plotted in figure 1 by red and blue lines respectively. Equations (7) and (8) can be expressed in a more general form for any arbitrary choice of energies s_1 and s_2 as

$$\lambda_q = \frac{f^{s_1}\lambda^{s_2} - f^{s_2}\lambda^{s_1}}{f^{s_1} - f^{s_2}}\,, \tag{9}$$

and

$$\lambda_g = \frac{\left(1-f^{s_2}\right)\lambda^{s_1} - \left(1-f^{s_1}\right)\lambda^{s_2}}{f^{s_1} - f^{s_2}}\,. \tag{10}$$

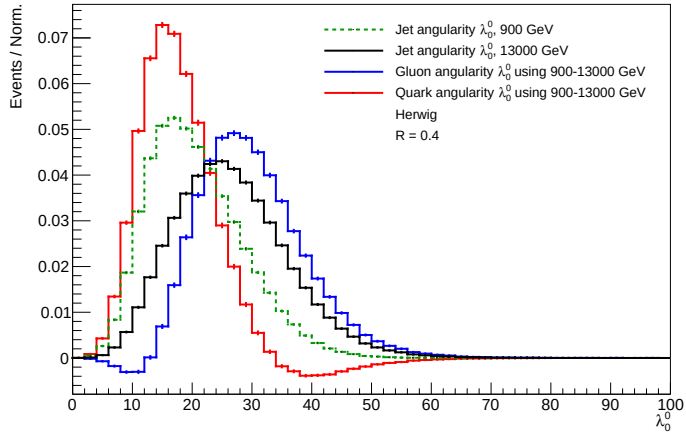

Fig. 1. Derived distributions of quark and gluon angularity (multiplicity) λ_q (red line) and λ_g (blue line) as linear combinations of those measured at different energies (green and black lines). Figure taken from [1].

4. Gluon fractions f^{s_1} and f^{s_2}

By disabling hadronization and parton showering in the Monte Carlo generators Herwig 7 and Pythia 8, the gluon fraction was defined as a function of p_{T}

$$f\left(p_{\mathrm{T}}\right) = \frac{N_{\mathrm{gluons}}\left(p_{\mathrm{T}}\right)}{N_{\mathrm{gluons}}\left(p_{\mathrm{T}}\right) + N_{\mathrm{quarks}}\left(p_{\mathrm{T}}\right)}\,, \tag{11}$$

where N represents the number of partons (quarks or gluons). In the left panel of figure 2, we show examples of gluon fractions as a function of transverse momentum $f(p_{\mathrm{T}})$ at $\sqrt{s} = 900$ GeV and 13000 GeV of Herwig (solid lines). In the right panel of figure 2, we show the p_{T} distributions of jets ($R = 0.4$) that passed the event selection cuts obtained by running a complete Monte Carlo simulation (including hadronization and parton shower) at two different collision energies of 900 and 13000 GeV. The transverse momentum mean $\langle p_{\mathrm{T}} \rangle$ of the jet distribution for the two energies is as follows:

— jet p_{T} ($\sqrt{s} = 900$ GeV) $\rightarrow \langle p_{\mathrm{T}} \rangle = 114.57$ GeV,
— jet p_{T} ($\sqrt{s} = 13$ TeV) $\rightarrow \langle p_{\mathrm{T}} \rangle = 125.63$ GeV.

The scaling coefficients f^{900} and f^{13000}, as illustrated by the dashed lines in figure 2, are obtained using the gluon fractions of the left panel at the $\langle p_{\mathrm{T}} \rangle$ derived from the right panel of figure 2

$$f^{900} = f^{900}\left(\langle p_{\mathrm{T}} \rangle\right) = f^{900}(114.57\ \mathrm{GeV}) = 0.33\,, \tag{12}$$
$$f^{13000} = f^{13000}\left(\langle p_{\mathrm{T}} \rangle\right) = f^{13000}(125.63\ \mathrm{GeV}) = 0.73\,. \tag{13}$$

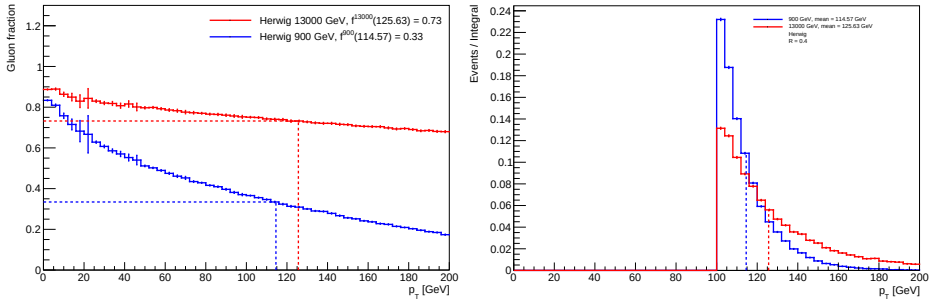

Fig. 2. Left panel: gluon fractions obtained from Herwig's simulation of the proton–proton dijet process without hadronization and parton showering at $\sqrt{s} = 900$ GeV f^{900} (blue solid line) and $\sqrt{s} = 13000$ GeV f^{13000} (red solid line). Dashed lines show the chosen values f^{900} and f^{13000} for the point at the mean of the jet p_{T} distributions. Right panel: Normalised transverse momentum of the leading and subleading jets at the energies of 900 and 13000 GeV. Dashed lines represent the mean of the distributions used to evaluate the coefficients of the gluon fraction. Figures taken from [1].

5. Results

In the left plot of figure 3, an example shows, similar to figure 1, the multiplicity λ_0^0 ($R = 0.4$, $p_{\mathrm{T}}^{\mathrm{cut}} = 100$) of the quark jets (red lines) and the gluon jets (blue lines). The plot includes angularities derived using all 6 energy combinations using full simulation, which are denoted by various types of lines. Additionally, the dots represent the angularities derived with MPI and ISR turned off. For simplicity, the right panel shows the same observable, solid lines representing the averaged q/g angularities across different energy combinations. The filled area builds the envelope of the different energy combinations, and the ticks represent the envelope of the statistical

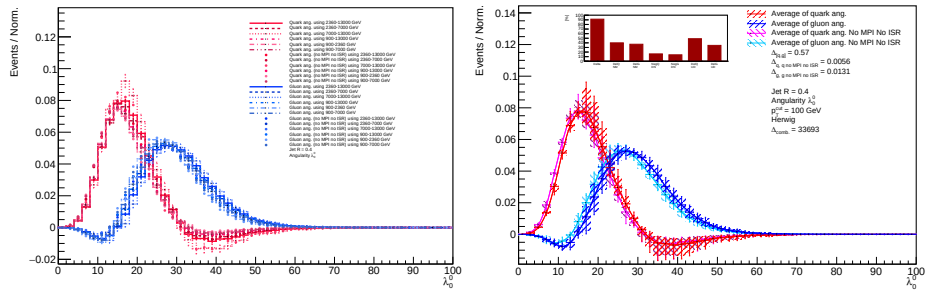

Fig. 3. Quark and gluon multiplicities λ_0^0 ($R = 0.4$, $p_{\mathrm{T}}^{\mathrm{cut}} = 100$) for all six energy combinations (above) and averaged plot showing the envelopes of the different energy combinations as filled areas and their statistical uncertainties as ticks (below). Figures taken from [1].

uncertainties of the angularities. By comparing this plot with the example in figure 1, one can gain additional insight into how the observables are robust to systematic effects.

Figures 4 (a)–(e) represent the best selection based on Δ_{comb} score [1] for each type of angularity. The score accounts for high separation power between quark and gluon angularities, low negativity, robustness to MPI and ISR effects, and energy independence of the angularities.

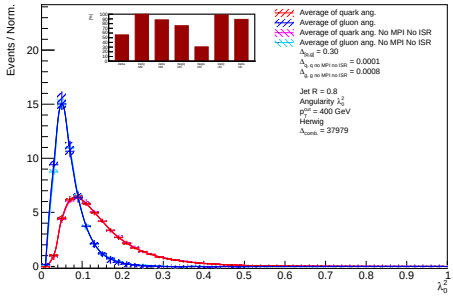

(a) p_{T}^{D} λ_0^2, $R = 0.8$, $p_{\text{T}}^{\text{cut}} = 400$

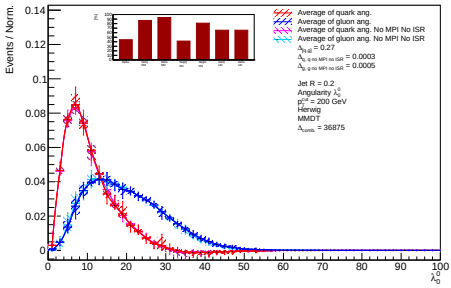

(b) Mult. λ_0^0, $R = 0.2$, $p_{\text{T}}^{\text{cut}} = 200$

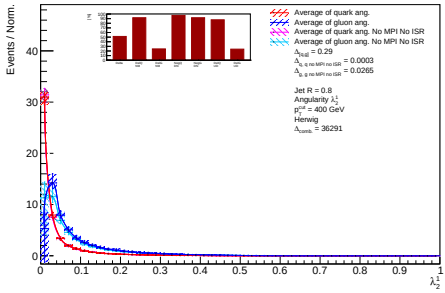

(c) Mass λ_2^1, $R = 0.8$, $p_{\text{T}}^{\text{cut}} = 400$

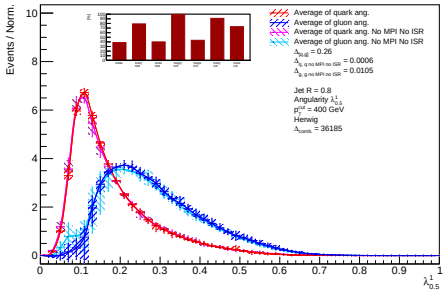

(d) LHA $\lambda_{0.5}^1$, $R = 0.8$, $p_{\text{T}}^{\text{cut}} = 400$

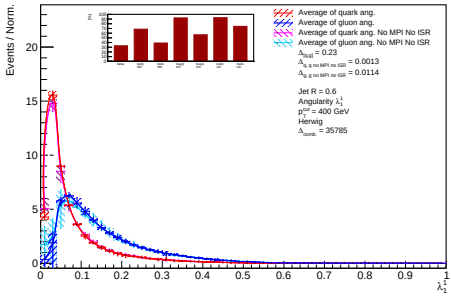

(e) Width λ_1^1, $R = 0.6$, $p_{\text{T}}^{\text{cut}} = 400$

Fig. 4. Quark and gluon averaged angularities derived using the Herwig event generator, using the average of 6 energy combinations 900–2360, 900–7000, 900–13000, 2360–7000, 2360–13000, and 7000–13000 GeV. Figures taken from [1].

6. Conclusion

The best-performing angularities presented in plots 4 (a)–(e) provide convincing evidence supporting the assumption that, for these angularities, quarks and gluons remain independent of collision energy. This conclusion is drawn from the relatively narrow envelope of the filled area, which represents angularities derived at different energy combinations. Plots show the independence of energy for higher-p_{T} jets except multiplicity with large-radius jets, where we found the uncertainties to be too high to be useful. We have shown that it is feasible and interesting to perform q/g-jet measurements based on the proposed method at the LHC at the energies of 7 (or 5) TeV and 13 TeV.

M.H.S. gratefully acknowledges funding from the U.K. Science and Technology Facilities Council (grant No. ST/T001038/1). The work of A.S. and P.B. is funded by grant No. 2019/34/E/ST2/00457 of the National Science Centre (NCN), Poland. P.B. is also supported by the Priority Research Area Digiworld under the program Excellence Initiative — Research University at the Jagiellonian University in Cracow and by the Polish National Agency for Academic Exchange NAWA under the Programme STER Internationalisation of doctoral schools, project No. PPI/STE/2020/1/00020.

REFERENCES

[1] P. Baroň, M.H. Seymour, A. Siódmok, *Eur. Phys. J. C* **84**, 28 (2024), arXiv:2307.15378 [hep-ph].

[2] A.J. Larkoski, J. Thaler, W.J. Waalewijn, *J. High Energy Phys.* **2014**, 129 (2014), arXiv:1408.3122 [hep-ph].

[3] J. Bellm *et al.*, *Eur. Phys. J. C* **76**, 196 (2016), arXiv:1512.01178 [hep-ph].

[4] J. Bellm *et al.*, *Eur. Phys. J. C* **80**, 452 (2020), arXiv:1912.06509 [hep-ph].

[5] L.A. Harland-Lang, A.D. Martin, P. Motylinski, R.S. Thorne, *Eur. Phys. J. C* **75**, 204 (2015), arXiv:1412.3989 [hep-ph].

[6] T. Sjöstrand *et al.*, *Comput. Phys. Commun.* **191**, 159 (2015), arXiv:1410.3012 [hep-ph].

[7] C. Bierlich *et al.*, arXiv:2203.11601 [hep-ph].

[8] R.D. Ball *et al.*, *Nucl. Phys. B* **877**, 290 (2013), arXiv:1308.0598 [hep-ph].

[9] M. Cacciari, G.P. Salam, G. Soyez, *J. High Energy Phys.* **2008**, 063 (2008), arXiv:0802.1189 [hep-ph].

[10] M. Cacciari, G.P. Salam, *Phys. Lett. B* **641**, 57 (2006), arXiv:hep-ph/0512210.

[11] M. Cacciari, G.P. Salam, G. Soyez, *Eur. Phys. J. C* **72**, 1896 (2012), arXiv:1111.6097 [hep-ph].

[12] J.M. Butterworth, A.R. Davison, M. Rubin, G.P. Salam, *Phys. Rev. Lett.* **100**, 242001 (2008), arXiv:0802.2470 [hep-ph].

[13] S.D. Ellis, C.K. Vermilion, J.R. Walsh, *Phys. Rev. D* **80**, 051501 (2009), arXiv:0903.5081 [hep-ph].

[14] S.D. Ellis, C.K. Vermilion, J.R. Walsh, *Phys. Rev. D* **81**, 094023 (2010), arXiv:0912.0033 [hep-ph].

[15] D. Krohn, J. Thaler, L.-T. Wang, *J. High Energy Phys.* **2010**, 084 (2010), arXiv:0912.1342 [hep-ph].

[16] M. Dasgupta, A. Fregoso, S. Marzani, G.P. Salam, *J. High Energy Phys.* **2013**, 029 (2013), arXiv:1307.0007 [hep-ph].

[17] A.J. Larkoski, S. Marzani, G. Soyez J. Thaler, *J. High Energy Phys.* **2014**, 146 (2014), arXiv:1402.2657 [hep-ph].